RevMexAA (Serie de Conferencias), **36**, CD272–CD277 (2009)

INFLUENCE OF THE MAGNETIC FIELD ON THE FORMATION OF POPULATION III STARS

M. N. Machida,[1] K. Omukai,[2] T. Matsumoto,[3] and S. Inutsuka[1]

RESUMEN

Estudiamos los flujos emergentes y los procesos de fragmentación en el colapso de nubes primordiales usando simulaciones MHD tridimensionales con mallas adaptivas. Empezando desde una densidad numérica de $n_{\rm c} \simeq 10^3\,{\rm cm}^{-3}$, seguimos la evolución de una nube esférica en rotación con un campo magnético uniforme hasta la densidad estelar $n_{\rm c} \simeq 10^{22}\,{\rm cm}^{-3}$. Calculamos 36 modelos parametrizando las energías magnéticas γ_0 y la de rotación β_0. En el colapso de nubes primordiales, la evolución de las nubes se caracterizan por la razón entre las energias rotacionales y magnéticas, γ_0/β_0. La fuerza de Lorentz afecta significativamente la evolución de las nubes con $\gamma_0 > \beta_0$, mientras que la fuerza centrífuga domina a la de Lorentz en nubes con $\beta_0 > \gamma_0$. Cuando las nubes rotan rápidamente con velocidad angular de $\Omega_0 > 10^{-17}\,{\rm s}^{-1}$ y $\beta_0 > \gamma_0$, la fragmentación ocurre antes de la formación de las protoestrellas, y no aparecen flujos emergentes después de la formación protoestelar. Por otra parte, aparecen fuertes flujos después de la formación protoestelar sin fragmentación cuando la nube inicial tiene un campo magnético fuerte de $B_0 > 10^{-9}$ G y $\gamma_0 > \beta_0$. Nuestros resultados indican que la estrellas de proto-población III muestran frecuentemente fragmentación y flujos protoestellares. Así, tanto como en la formación estelar del presente, las estrellas de población III nacen como binarias o como sistemas estelares múltiples, produciendo fuertes flujos lo cuales alteran significativamente el medio interestelar e inducen la formación de la siguiente generación estelar.

ABSTRACT

Outflow and fragmentation processes in collapsing primordial cloud are studied using three-dimensional MHD nested grid simulations. Starting from the number density of $n_{\rm c} \simeq 10^3\,{\rm cm}^{-3}$, we follow the evolution of rotating spherical cloud with uniform magnetic field up to the stellar density $n_{\rm c} \simeq 10^{22}\,{\rm cm}^{-3}$. We calculate 36 models parameterizing the magnetic γ_0 and rotational β_0 energies. In the collapsing primordial clouds, cloud evolutions are characterized by the ratio of the rotational to magnetic energy, γ_0/β_0. The Lorentz force significantly affects the cloud evolution in the cloud with $\gamma_0 > \beta_0$, while the centrifugal force is more dominant than the Lorentz force in the cloud with $\beta_0 > \gamma_0$. When the cloud rotates rapidly with angular velocity of $\Omega_0 > 10^{-17}\,{\rm s}^{-1}$ and $\beta_0 > \gamma_0$, fragmentation occurs before the protostar formation, but no outflow appears after the protostar formation. On the other hand, strong outflow appears after the protostar formation without fragmentation when the initial cloud has the strong magnetic field of $B_0 > 10^{-9}$ G and $\gamma_0 > \beta_0$. Our results indicate that proto-Population III stars frequently show fragmentation and protostellar outflow. Thus, as well as the present-day star formation, Population III stars are born as the binary or multiple stellar system, and they can drive strong outflow which significantly disturb the interstellar medium and may induce the formation of next generation stars.

Key Words: early-universe — ISM: jets and outflows — MHD — stars: formation

1. INTRODUCTION

Magnetic field has an important role in present-day star formation. Observations indicate that molecular clouds have the magnetic field strengths of order $\sim \mu$G and magnetic energies comparable to the gravitational energies (Crutcher 1999). These strong fields significantly affect the star formation process. For example, protostellar jet, which is ubiquitous phenomena in the star-forming region, is considered to be driven from the protostar by the Lorentz force (Blandford & Payne 1982). The jet influences the gas accretion onto the protostar and disturbs the ambient medium. In addition, the angular momentum of the cloud is removed by the magnetic effect:

[1]Department of Physics, Graduate School of Science, Kyoto University, Sakyo-ku, Kyoto 606-8502, Japan (machidam@scphys.kyoto-u.ac.jp, inutsuka@tap.scphys.kyoto-u.ac.jp).

[2]National Astronomical Observatory of Japan, Mitaka, Tokyo 181-8588, Japan (omukai@th.nao.ac.jp).

[3]Faculty of Humanity and Environment, Hosei University, Fujimi, Chiyoda-ku, Tokyo 102-8160, Japan (matsu@i.hosei.ac.jp).

the magnetic braking and protostellar jet. Tomisaka (2000) showed that, in his two dimensional MHD calculation, 99.9% of the angular momentum is transferred from the center of cloud by the magnetic effect. This removal process of angular momentum makes the protostar formation possible in the parent cloud that has much larger specific angular momentum than the protostar. On the other hand, so far, the magnetic effects in the primordial gas cloud have been ignored, because the magnetic field in the early universe is considered to be extremely weak if it exists. However, recent studies indicate moderate strength of the magnetic field in the early universe. Ichiki et al. (2006) showed that cosmological fluctuations produce magnetic fields before the epoch of recombination. These fields are large enough to seed the magnetic fields in galaxies. Langer et al. (2003) proposed the generation mechanism of magnetic fields at the epoch of the reionization of the universe. They found that magnetic fields in the intergalactic matter are amplified to $\sim 10^{-11}$ G. Thus, these fields can increase up to $\simeq 10^{-7} - 10^{-8}$ G in the first collapsed object having $n \sim 10^3\,\mathrm{cm}^{-3}$ of the number density. These fields may influence the evolution of primordial gas clouds and the formation of Population III stars.

In this paper, we investigate the evolution of weakly magnetized primordial clouds and formation of Population III stars using three-dimensional MHD simulations, and show the driving condition of outflow from proto-Population III stars and fragmentation condition in the collapsing primordial cloud.

2. MODEL

Our initial settings are almost the same as those of Machida et al. (2006b, 2007). To study the cloud evolution, we use the three-dimensional ideal MHD nested grid code. We solve the MHD equations including the self-gravity:

$$\frac{\partial \rho}{\partial t} + \nabla \cdot (\rho \boldsymbol{v}) = 0\,, \quad (1)$$

$$\rho \frac{\partial \boldsymbol{v}}{\partial t} + \rho(\boldsymbol{v} \cdot \nabla)\boldsymbol{v} = -\nabla P - \frac{1}{4\pi}\boldsymbol{B} \times (\nabla \times \boldsymbol{B}) - \rho \nabla \phi\,, \quad (2)$$

$$\frac{\partial \boldsymbol{B}}{\partial t} = \nabla \times (\boldsymbol{v} \times \boldsymbol{B})\,, \quad (3)$$

$$\nabla^2 \phi = 4\pi G \rho\,, \quad (4)$$

where ρ, $\boldsymbol{v}$, P, $\boldsymbol{B}$, and ϕ denote the density, velocity, pressure, magnetic flux density, and gravitational potential, respectively. For gas pressure, we use a barotropic relation that approximates the result of Omukai et al. (2005). As the initial condition of the cores, we use the critical Bonnor-Ebert density profile. As the initial state, we adopted the number density as $n_{c,0} = 1.86 \times 10^3\,\mathrm{cm}^{-3}$, and the initial temperature as 250K at the center of cloud. The critical radius of the Bonnor-Ebert sphere is $R_\mathrm{c} = 6.5\,\mathrm{pc}$. The total mass contained in the critical Bonnor-Ebert sphere is $M_\mathrm{c} = 1.8 \times 10^4\,M_\odot$. Initially the cloud rotates rigidly Ω_0 around the z-axis and has a uniform magnetic field B_0 parallel to the z-axis (or rotation axis). The initial model is characterized by two nondimensional parameters: the ratio of the rotational β_0 ($E_\mathrm{r}/E_\mathrm{g}$), and magnetic energy γ_0 ($E_\mathrm{b}/E_\mathrm{g}$) to the gravitational energy, where E_r, E_b and E_g are the rotational, magnetic, and gravitational energies of the initial cloud. We made 36 models by combining these two parameters. To promote fragmentation, we add $m = 2$-mode axisymmetric density perturbation to the initial cores.

We adopt the nested grid method (for details, see Machida et al. 2005a, 2006a) to obtain high spatial resolution near the center. Each level of a rectangular grid has the same number of cells ($= 128 \times 128 \times 64$), with the cell width $h(l)$ depending on the grid level l. The cell width is halved with every increment of the grid level. The highest level of grids changes dynamically: a new finer grid is generated whenever the minimum local Jeans length λ_J falls below $8\,h(l_\mathrm{max})$, where h is the cell width. The maximum level of grids is restricted to $l_\mathrm{max} = 30$. Since the density is highest in the finest grid, the generation of a new grid ensures the Jeans condition of Truelove et al.(1997) with a margin of a safety factor 2.

2.1. *Cloud Fragmentation*

Figure 1 shows final state on $z = 0$ plane in each model against initial magnetic (γ_0, x-axis) and rotational energies (β_0, y-axis). In Figure 1, models are classified into four types: fragmentation models (blue), non-fragmentation models (red), merger models (green) in which the fragments merge after fragmentation, and no collapsing model (gray). The fragmentation models are distributed in the upper left region, which indicates that fragmentation is easy to occur when the initial cloud has a weaker magnetic field and more rapid rotation. Namely, the magnetic field suppresses fragmentation, while the cloud rotation promotes fragmentation.

Figure 1 also shows that fragmentation and non-fragmentation models are clearly separated: fragmentation occurs in the upper left region (models with more rapid rotation and weaker magnetic field), while fragmentation does not occur in the lower right region (models with slower rotation and stronger

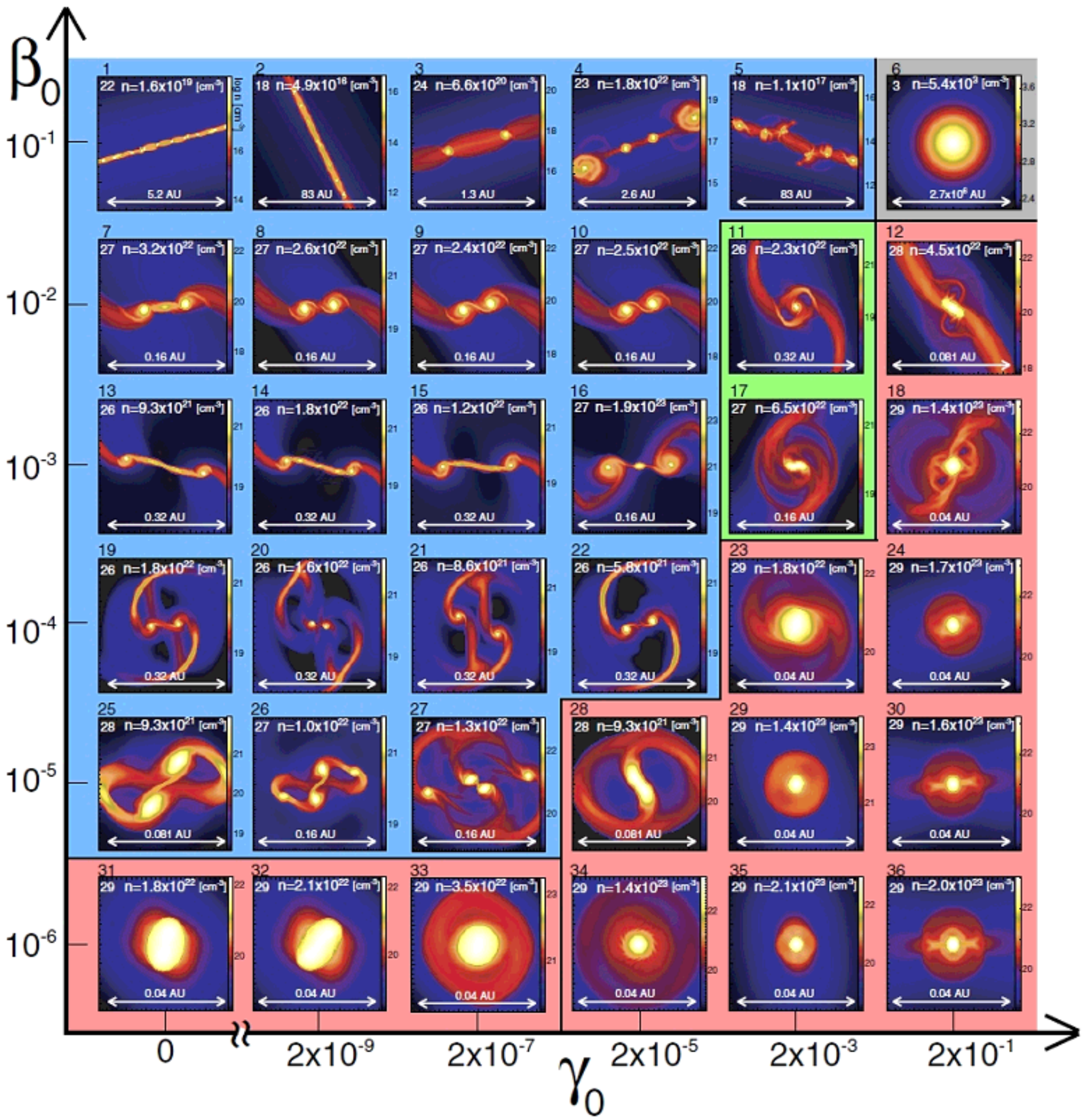

Fig. 1. Final states on the $z = 0$ plane against parameters γ_0 and β_0. The model numbers are described in the upper left corner outside each panel. The density distribution (color-scale) is plotted in each panel. The grid level, maximum number density (n), and grid scale are denoted inside each panel. Background colors, respectively, indicate the fragmentation (*blue*), non-fragmentation (*red*), merger (*green*), and no-collapse (*gray*) models.

magnetic field). In addition, merger models are distributed at the border between fragmentation and non-fragmentation models. In fragmentation models, models with weaker magnetic field and more rapid rotation tend to have wider separation. On the other hand, in non-fragmentation models, clouds have more compact cores in models with stronger magnetic fields and slower rotations. These features clearly indicate that the rotation promotes fragmentation but the magnetic field suppresses fragmentation even in primordial star formation, as well as the present-day star formation (Hosking & Whitworth 2004; Machida et al. 2004, 2005b, 2008a; Price & Bate 2007; Hennebelle & Teyssier 2008). We added a small amount of the non-axisymmetric density perturbation ($A_\phi = 0.01$) to the initial state. When the initial cloud is largely distorted, fragmentation region might not be clearly separated. However, Machida et al. (2008a) showed that the initial amplitude of the non-axisymmetric perturbation does not qualitatively depend on the fragmentation condition in the collapsing cloud. Moreover, Machida et al. (2008b) showed that fragmentation condition in collapsing primordial cloud slightly depend on the initial amplitude of the non-axisymmetric perturbation. Thus, we expect that the initial amplitude of the non-axisymmetric perturbation hardly affect the fragmentation condition even in the primordial magnetized collapsing cloud.

2.2. *Outflow and Magnetic Field Lines*

After the protostar formation, outflow appears in some models (outflow models). In all the outflow models, outflow appears only after the protostar is formed. Because the rotational timescale of cloud becomes shorter than the collapse timescale after the protostar formation, the magnetic field lines begin to be twisted and outflow appears. Figure 2 shows the configuration of the magnetic field lines (black-white streamlines) and structure of outflow (transparent red iso-velocity surface) for each model.

In the outflow models in Figure 2, the magnetic field lines are strongly twisted inside the outflow. Since we added the non-axisymmetric density perturbation to the initial state, some models show the non-axisymmetric circumstellar disks, which are represented by a red iso-density surface in Figure 2. In Figure 2, almost axisymmetric hourglass-like outflows are seen in models 18, 23, 24, 28, 29, 34, and 35, while non-axisymmetric outflows are seen in models 17, 30, and 36. Non-axisymmetric structure of outflow is caused by the non-axisymmetric density pattern at the protostar formation epoch. Thus, when the non-axisymmetric perturbation sufficiently grows before the protostar formation, the non-axisymmetric outflow appears. For example, in model 30, the non-axisymmetric outflow (transparent red iso-velocity surface) is driven from bar-like density distribution (red iso-density velocity surface) in the root of the outflow.

After fragmentation, the configuration of the magnetic field lines are changed. When fragmentation does not occur, central region has hourglass-like configuration of the magnetic field lines, in which poloidal component is more dominant than the toroidal component. These configurations of the magnetic field lines can easily drive the outflow by the disk wind mechanism (Blandford & Payne 1982). On the other hand, when fragmentation occurs, the toroidal field tends to be more dominant than the poloidal filed. Under these configurations, it is difficult to drive the outflow, because the outflow loses the place to go when the magnetic field lines are not aligned to the rotation axis. Note that strong toroidal field has advantage for fragmentation, because the magnetic tension force and magnetic pressure may suppress merger of fragments as shown in Price & Bate (2007). In our calculation, any fragmentation model did not show the outflow. These models have larger rotational but smaller magnetic energies at initial stage. In addition, the growth rate of the magnetic field becomes small in these models. Thus, we cannot determine the reason why no outflows appear in these models: because of configuration of the magnetic field lines due to fragmentation, or because of initially weak magnetic field and small growth rate of the magnetic field. However, after fragmentation, the poloidal component grows as time and the outflow may be driven from the protostar in further evolution. Model 22 in Figure 2 shows that each fragment has a strong toroidal and poloidal field, which is caused by the spin motion of each fragment.

3. SUMMARY

In this study, to investigate the magnetic effect in the collapsing primordial cloud, we calculated cloud evolution from $10^3\,\mathrm{cm}^{-3}$ until the protostar is formed ($\simeq 10^{22}\,\mathrm{cm}^{-3}$) for 36 models, in which initial magnetic and rotational energies are parameterized. We found that fragmentation occurs in the collapsing cloud but no outflow appears after the protostar is formed, when $\beta_0 > \gamma_0$. On the other hand, when $\beta_0 < \gamma_0$, outflow appears after the protostar formation without fragmentation. As a result, in the collapsing primordial cloud, the cloud evolution is mainly controlled by the centrifugal force than the Lorentz force when $\beta_0 > \gamma_0$, while the Lorenz force is more dominant than the centrifugal force when $\gamma_0 > \beta_0$.

Outflow can be driven by the protostar when the initial cloud has $B_0 \gtrsim 10^{-9}\,\mathrm{G}$ of the magnetic field if the cloud rotates slowly ($\omega \lesssim 4\times10^{-17}\,\mathrm{s}^{-1}$), whose condition corresponds to that in Machida et al. (2006b). Since we calculated the evolution of outflow only for several days for numerical limitation, we cannot estimate the mass ejection rate and final speed of outflow. In present-day star formation, the mass ejection rate by outflow is 1/10 of the mass accretion, and outflow stops after mass accretion stops. In primordial star formation, the accretion rate is expected to be considerably larger than that

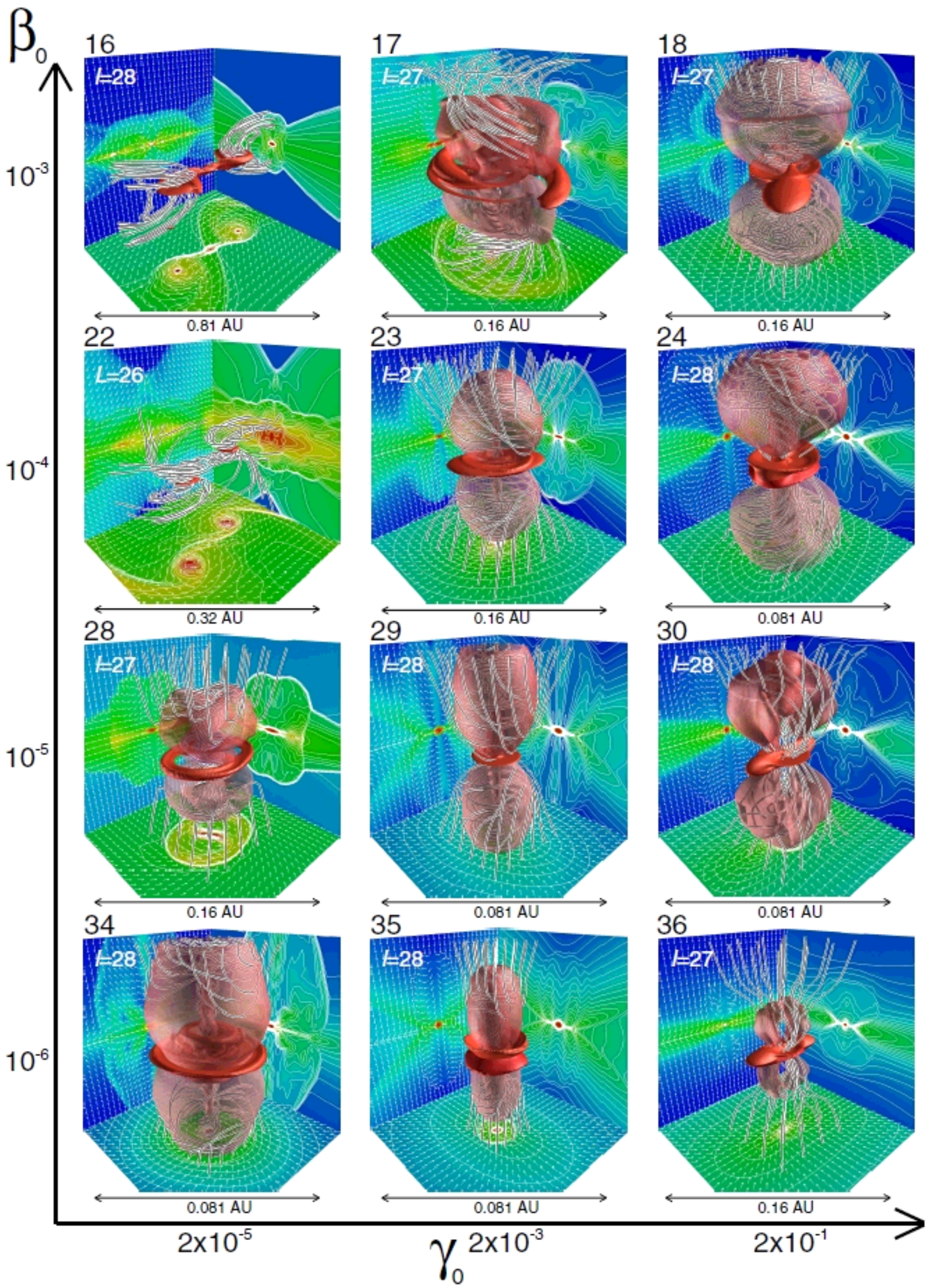

Fig. 2. Final states in three dimensions against parameters γ_0 and β_0. The model numbers are described in the upper left corner outside each panel. The magnetic field lines (*black and white streamlines*), high-density region (*red isosurface*), and outflow region (*transparent red isosurface*) are plotted in each panel. The density contours (*false color* and *contour lines*) and velocity vectors (*thin arrows*) are also projected in each wall surface. The grid level, and grid scale are shown in each panel.

at present day. This large accretion rate may make a strong outflow (or jet). Omukai & Palla (2001, 2003) showed that, for Population III stars, the gas accretion does not halt for their lifetimes. Thus, outflows also may continue for their lifetimes and propagate to disturb surrounding medium significantly. On the other hand, when the magnetic field strength of initial cloud is weaker than $B_0 < 10^{-9}$ G, the magnetic effect can be ignored at least before the protostar formation. When $B_0(n_c/10^3\,\mathrm{cm}^{-3})^{2/3}$ is assumed, the critical magnetic field strength $B_0 = 10^{-9}$ G at $n = 10^3\,\mathrm{cm}^{-3}$ can be converged to the background value of $B_{0,\mathrm{b}} = 5 \times 10^{-13}$ G ($n = 0.01\,\mathrm{cm}^{-3}$), which is much stronger than the magnetic field derived by Ichiki et al. (2006). However, when the magnetic field is amplified to $B > 10^{-9}(n/10^3\,\mathrm{cm}^{-3})^{2/3}$ G by any mechanism, the magnetic field can affect the evolution of the primordial cloud. In addition, since we calculated the cloud evolution for a short duration ($\sim$ days) after the protostar formation, the protostar and circumstellar disk is influenced by the magnetic field even in the cloud with $B_0 < 10^{-9}$ G in a subsequent accretion phase.

The angular velocity affects the evolution of the primordial cloud when the first collapsed objects ($n_c \simeq 10^3\,\mathrm{cm}^{-3}$) has $\Omega_0 \gtrsim 10^{-17}\,\mathrm{s}^{-1}$ of the angular velocity, in which fragmentation can occur and binary or multiple stellar system is expected to be born. When the multiple stellar system is formed, some star can be ejected by close encounter. At the protostar formation epoch, the protostar has a mass of $M \simeq 10^{-3}\,M_\odot$. Thus, ejected proto-Population III stars may evolve to metal-free brown dwarfs or low-mass stars. When the binary component in multiple stellar system is ejected from parent cloud by protostellar interaction, low-mass metal free binary may also be appeared in the early universe. Suda et al. (2004) indicated that the extremely metal-poor ([Fe/H]< -4) stars are formed as binary members from metal-free gas, and then have been polluted by companion stars during the stellar evolution. Komiya et al. (2006) showed that binary frequency in Population III star is comparable to or larger than that at present day. However, since we calculated the cloud evolution just after fragmentation, we need to further long-term calculation to determine whether fragments evolve to binary or multiple stellar system.

REFERENCES

Blandford, R. D., & Payne, D. G. 1982, MNRAS, 199, 883
Crutcher R. M. 1999, ApJ, 520, 706
Hosking, J. G., & Whitworth, A. P., 2004, MNRAS, 347, 3
Ichiki, K., Takahashi, K., Ohno, H., Hanayama, H., & Sugiyama, N. 2006, Science, 311, 787
Komiya, Y., Suda, T., Minaguchi, H., Shigeyama, T., Aoki, W., & Fujimoto, M. Y. 2007, ApJ, 658, 367
Langer, M., Puget, J.-L., & Aghanim, N. 2003, Phys. Rev. D, 67, 043505
Hennebelle, P., & Teyssier, R., 2008, A&A, 477, 25)
Machida, M. N., Tomisaka, K., & Matsumoto, T. 2004, MNRAS, 348, L1
Machida, M. N., Matsumoto, T., Tomisaka, K., & Hanawa, T. 2005a, MNRAS, 362, 369
Machida, M. N., Matsumoto, T., Hanawa, T., & Tomisaka, K. 2005b, MNRAS, 362, 382
Machida, M. N., Matsumoto, T., Hanawa, T., & Tomisaka, K. 2006a, ApJ, 645, 1227
Machida, M. N., Omukai, K., Matsumoto, T., & Inutsuka, S. 2006b, ApJ, 647, L1
Machida, M. N., Inutsuka, S.-I., & Matsumoto, T. 2007, ApJ, 670, 1198
Machida, M. N., Tomisaka, K., Matsumoto, T., & Inutsuka, S. 2008a, ApJ, 677, 327
Machida, M. N., Omukai, K., Matsumoto, T., & Inutsuka, S. 2008b, ApJ, 677, 813
Omukai, K., & Palla, F. 2001, ApJ, 561, L55
———. 2003, ApJ, 589, 677
Omukai, K., Tsuribe, T., Schneider, R., & Ferrara, A. 2005, ApJ, 626, 627
Price, D. J., & Bate, M. R. 2007, MNRAS, 377, 77
Suda, T., Aikawa, M., Machida, M. N., Fujimoto, M. Y., & Iben, I. J. 2004, ApJ, 611, 476
Tomisaka, K. 2000, ApJ, 528, L41